Proceedings Paper:

Sun, G., Mitchell, R., Chen, Z. et al. (4 more authors) (2024) 3D characterisation of local deformation and damage development in tailored fibre placement-manufactured composites under tensile loading. In: Proceedings of SAMPE Europe 24. SAMPE Europe Conference & Exhibition 2024, 24-26 Sep 2024, Belfast, Northern Ireland. SAMPE Europe / Curran Associates , pp. 1050-1058. ISBN 9798331308292

1. 3D CHARACTERISATION OF LOCAL DEFORMATION AND DAMAGE DEVELOPMENT IN TAILORED FIBRE PLACEMENT-MANUFACTURED COMPOSITES UNDER TENSILE LOADING

Guowen Sun[a], Ria L Mitchell[a,b], Zilei Chen[a], Matt Smith[c], Fatma Omrani[c] , Patrick Fairclough[a], Christophe Pinna[a]

[a]*Department of Mechanical Engineering, The University of Sheffield, Sheffield S1 3JD, UK*
[b]*Department of Materials Science and Engineering, The University of Sheffield, UK, now at ZEISS microscopy*
[c]*Composites Centre, AMRC with Boeing, University of Sheffield, Sheffield S60 5ZT, UK*

ABSTRACT

The tensile response of Carbon Fibre Reinforced Polymer (CFRP) composites manufactured through Tailored Fibre Placement (TFP) has been investigated using micro X-ray computed tomography (µXCT) with in-situ mechanical testing combined with digital volume correlation (DVC). Damage mechanisms have been studied in relation to full-field strain measurements through regular interruptions of the tests and post-processing of the reconstructed images of the internal structure of the composite using a new Python-based DVC algorithm. A global DVC strategy has been developed to obtain deformation fields based on the correction of large rigid-body motions from a local DVC approach. Results show quantified strain distributions and their evolution in the complex 3D structure of the textile composite, in particular in resin-rich regions around stitch threads affecting damage development. The developed methodology therefore offers new opportunities for a better understanding of complex damage development in TFP composites as well as validation means for multiscale models aimed at predicting their mechanical response.

2. INTRODUCTION

Carbon Fibre Reinforced Polymers (CFRPs) composites are increasingly used in aerospace structures due to their inherent high strength and stiffness to weight ratio. Multi-layer laminates are often required to provide sufficient load bearing capacity and resistance to multi-directional loads. However, their thickness and the overall design of complex composite structures need to be optimised to reduce weight and machining-related material waste in order to meet net-zero targets. The concept of variable fibre path composites was generated for this purpose to minimise material waste without reducing load bearing capacity.

The tailored fibre placement (TFP) manufacturing process was developed to strategically locate fibre tows along desirable fibre paths in multiple directions. The principle of TFP is shown in Figure 1 [1]. An embroidery-type machine was adopted to manufacture a preform through stitching fibre tows on a base material. Fibre tows can be placed in any orientations using a 360° head-controlled rotation.

TFP applications are constantly growing, including for brake boosters [2] and bicycle frames [3], but better understanding of the effect of manufacturing parameters, such as stitch length, stitch width and roving distances, on mechanical performance is needed [4, 5]. The deformation of a TFP-made composite sample was studied under tensile loading using two-dimensional Digital Image Correlation (2D DIC) in [5]. Strain concentration was observed in resin-rich zones created by stitch-threads but the investigation was limited to surface measurements and cannot fully characterise strain distributions in the complex 3D structure of TFP composites.

Digital Volume Correlation (DVC) is a 3D strain field measurement method extended from 2D DIC. This approach was initially proposed by Bay et al. for strain measurement of trabecular bone tissue under compression loads [6]. Recently, DVC has been developed for investigating the internal deformation of composite materials under flexural loads [7, 8] or under tension [9].

In the current study, an in-situ tensile test was carried out on a TFP composite sample inside an X-ray Computed Tomography (XCT) microscope. The test was regularly interrupted to study both morphological changes of the internal structure and crack development. The internal deformation of the TFP composite sample was subsequently characterised through full-field strain distributions computed using a Python-coded DVC algorithm.

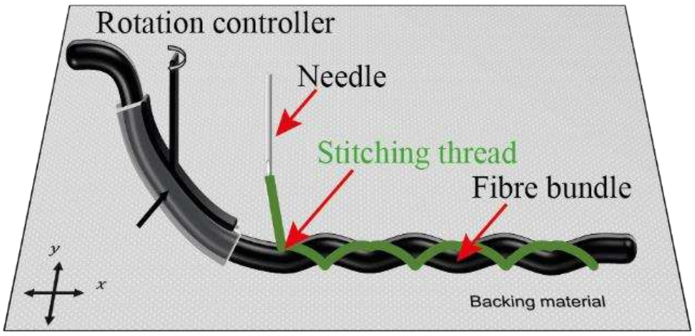

Figure 1: Principle of the TFP technique [1].

3. EXPERIMENTATION

3.1 Materials and specimens

TORAY carbon fibre tows, 800 tex and 12 K filament, were adopted for the TFP-preform fabrication. Serafil Comphil 180 polymer was selected for the thread to stitch the carbon fibre tows on a glass-fibre weave. A TFP composite made with a $[0/60/\text{-}60]_s$ layer sequence was manufactured by using Resin Transfer Moulding (RTM). The selected epoxy resin was LY564 with Aradur 5945 hardener. The thickness of the TFP composite laminate was 3.6 mm. A dog-bone shaped sample (Figure 2(a)) was then produced using waterjet cutting. A narrow width of 3 mm and a gauge length of 4 mm was designed to concentrate the deformation in the field of view (FOV) of XCT experiments.

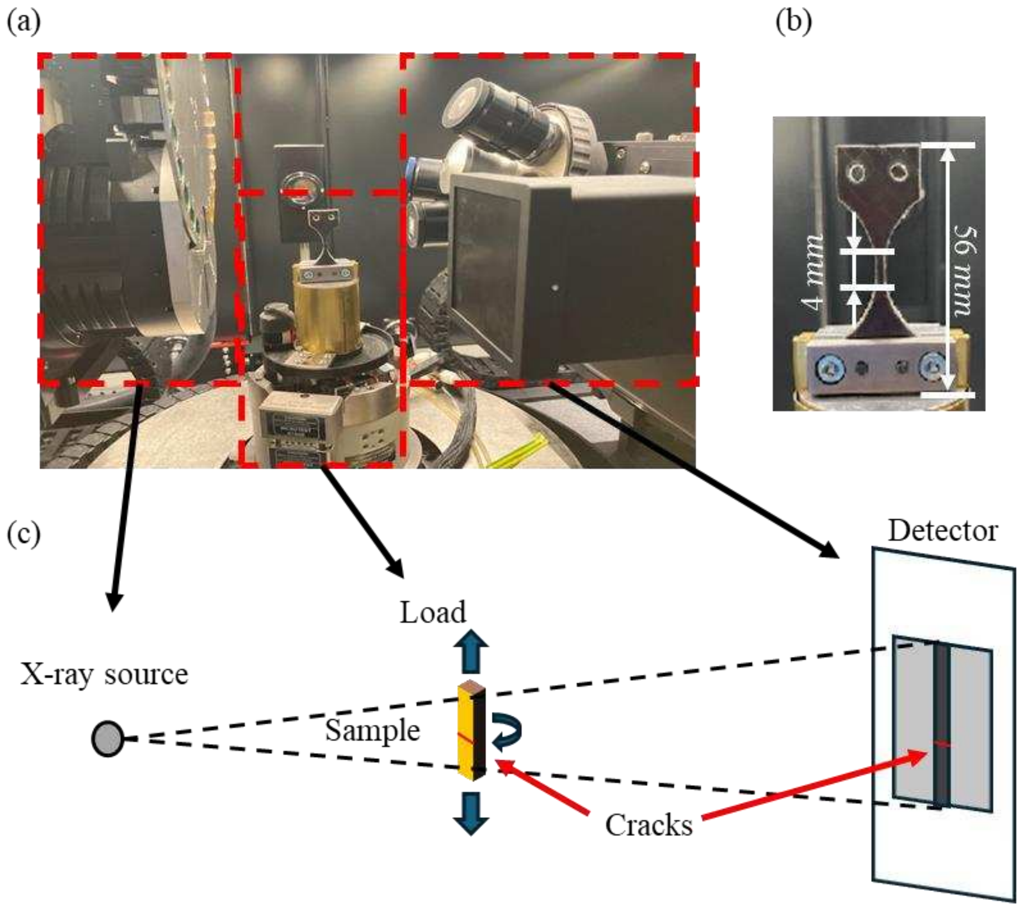

Figure 2: (a) Experimental setup in the CT scanner; (b) TFP composite specimen; (c) working configuration for the in-situ tensile test in the Versa 620 X-ray Microscope (XRM).

3.2 Experimental method and image segmentation

The in-situ tensile test was carried out at the Sheffield Tomography Centre, The University of Sheffield. A ZEISS Xradia 620 Versa X-ray Microscope (XRM) was used to inspect the internal structure of the TFP composite. The X-ray source voltage and power were set to 150 kV and 23 W respectively. A 0.4× objective lens was adopted to obtain a voxel size of 11.34 μm. 1601 projections were collected per scan, lasting about 1 hour. The collected data were further reconstructed into 8-bit tiff images for DVC characterization.

Eight scans were conducted for collecting information under different loading states as detailed in Table 1. Two reference scans of the unloaded TFP composite sample were included for noise investigation in the DVC analysis. Tensile tests were carried out using a 5 kN Deben CT5000TEC loading stage as shown in Figure 2(a). The loading rate was set as 0.5 mm/min.

Table 1: Load values and stress-to-failure ratios for the interrupted in-situ test

Load steps	Step 0	Step 1	Step 2	Step 3	Step 4	Step 5	Step 6

σ/σ_{UTS}	0	25%	37%	50%	75%	90%	95%
Load (kN)	0	0.93	1.31	1.86	2.8	3.36	3.54

The internal structure of the TFP composite sample was segmented from XCT results using Dragonfly ORS [13]. The segmented results of fibre bundles in each layer were further exported as STL mesh files. The open-source software, ParaView [14], was adopted for the visualisation of DVC results. With mesh files created from image segmentation results of the internal structure of the TFP composite, strain fields were mapped onto the mesh model to better understand the strain concentrations in the fibre bundle structure.

3.3 Python-coded DVC methods

Two main methods can be used for DVC, namely the subset-based local DVC (L-DVC) approach and the finite-element-based global DVC (G-DVC or FE-DVC) approach. The L-DVC method was adopted for dividing the volumetric images into individual subsets and searching for optimal similarity between the subsets from the reference and deformed images. The G-DVC method considered the entire subsets (grids) based on finite elements for displacement interpolation, which ensured displacement continuity.

The zero-mean normalized sum-of-square difference (ZNSSD) function was adopted as correlation function [10]:

$$C_{ZNSSD}(\Delta\mathbf{p}) = \sum_{\xi} \left\{ \frac{[f(\mathbf{x} + \mathbf{W}(\boldsymbol{\xi}; \Delta\mathbf{p})) - f_m]}{\Delta f} - \frac{[g(\mathbf{x} + \mathbf{W}(\boldsymbol{\xi}; \Delta\mathbf{p})) - g_m]}{\Delta g} \right\}^2 \quad (1)$$

where f_m and g_m are the mean greyscale values of the subvolumes in reference and deformed images respectively. $\Delta\mathbf{p}$ represents the incremental deformation vector.

The displacement-searching strategy used in the current model was the inverse-compositional Gauss-Newton (ICGN) algorithm. It was proposed for high-efficiency computation, high-robustness and accuracy for DIC by Pan et al. [11]. The ICGN algorithm was further utilised for 3D DVC for high-resolution image volume correlation with up to billions of voxels [12]. Considering the user-friendly and gradually popular programming language of Python, both L-DVC and G-DVC methods were programmed in a Python script using the ICGN iteration strategy.

4. RESULTS AND DISCUSSION

DVC was successfully conducted between every successive scanning steps. Three directional displacement fields (u, v and w) were obtained along the $x, y,$ and z directions respectively. The loading direction was along the z direction, while the through-thickness direction and the transversal direction of TFP composite specimen were aligned with the x and y directions respectively. Before the implementation of the sub-voxel DVC methods, the translational rigid body motion (RBM) had to be removed to improve the precision and efficiency of DVC results [15, 16].

4.1 Correlation of rigid body motion

Two methods were adopted for the detection of the translational RBM of X-ray scan results for the TFP composite sample under tension. The first method was based on the L-DVC method to obtain the correlated displacement fields. The correlation was carried out between every successive load-scan steps. Figure 7 (a) shows the accumulated RBM values obtained from the correlation results. Four different subset sizes (31, 41, 51 and 61 voxels) were selected. Limited differences in RBM values are observed along the x- and y- axes for these different subset sizes, whereas a larger, albeit not significant, difference in RBM values is found for the z directional displacement.

The second method was based on image processing. A region of interest (ROI) was selected from CT images and was assumed to remain the same for all loading scans. An image segmentation method was adopted for extracting those ROIs for each loading scans and exporting them as binary images separately. The centroid position of this ROI was extracted along three directions. Then the position difference was calculated between two loading steps and defined as the rigid body motion as shown in Figure 7 (b). The rigid body motions detected from the local DVC approach along the three directions were compared to those obtained from the image processing approach detailed above. A good agreement can be found along all three x, y, and z directions.

As shown in Figure 7, the x-directional RBM values remain positive during all loading steps, while y-directional RBM (transversal direction) values show both positive and negative values. The accumulated RBM along the transversal direction was back to its original position on step 5, while a high value can be found for the correlation between step 5 and step 6, which is assumed to be caused by the high density of cracks in the final loading step. The accumulated rigid body motion along the through-thickness direction was calculated as 23.62 voxels (267.85 μm) from the correlation results with a subset size of 61 voxels. Such a high accumulated rigid body motion was primary caused by the asymmetrical layup of the TFP composite preform. Due to the base material and stitch thread adopted for the TFP process, an extra layer of base material and a resin-rich layer were formed in the composite due to the hybrid stitch thread beneath the base material [1]. This asymmetry resulted in a coupled bending behavior for the TFP composite sample loaded under tension, which was captured in the X-ray CT results, with a partial rigid body motion and a partial internal bending deformation. The rigid body motion value for each subset calculated by the L-DVC method was saved and imported to the G-DVC algorithm for the further sub-voxel correlation.

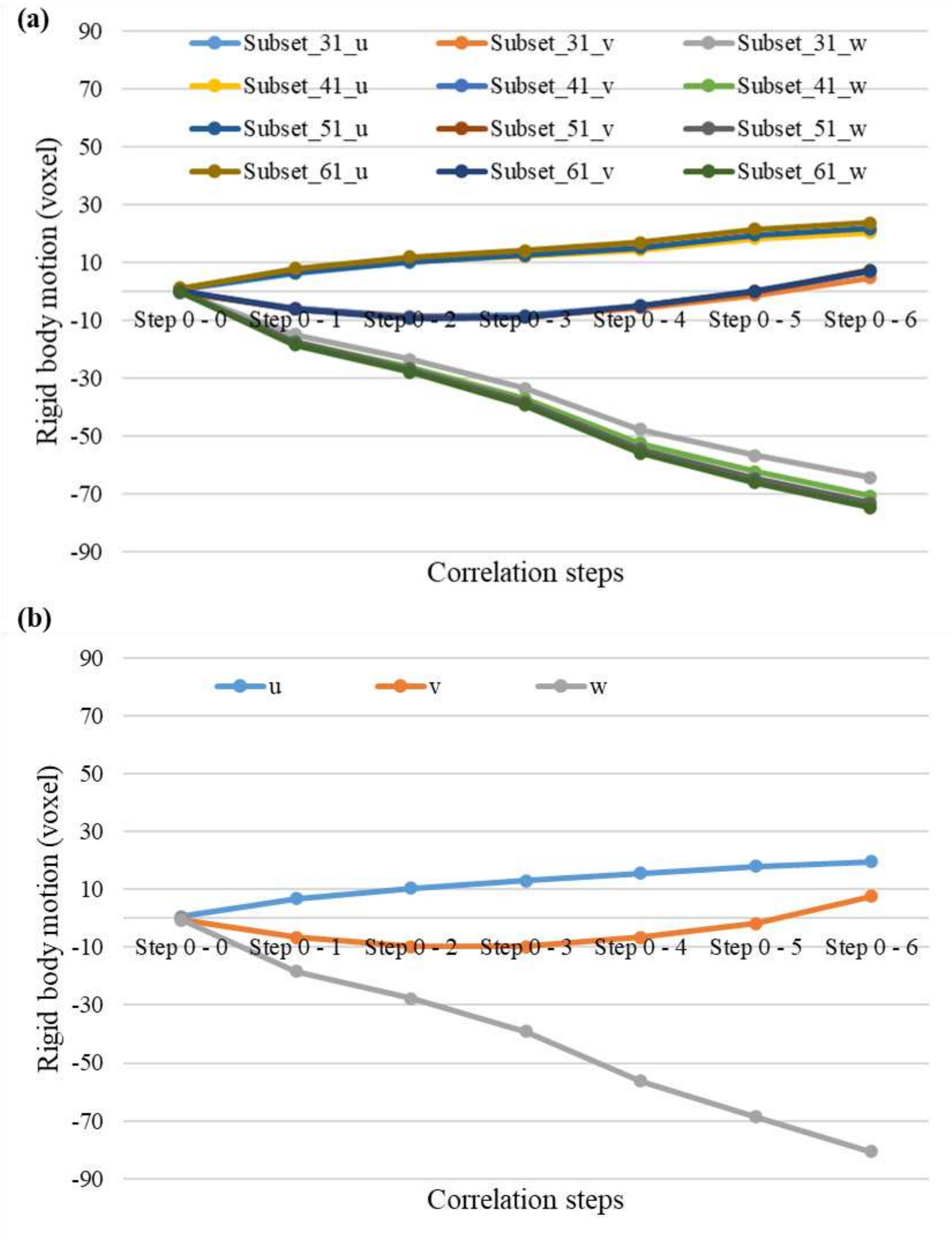

Figure 7: Three directional rigid body translations (u, v and w along x, y and z axes) detected from (a) Local DVC approach (for three particular subsets 31,41,51 and 61), and (b) Image processing using ImageJ.

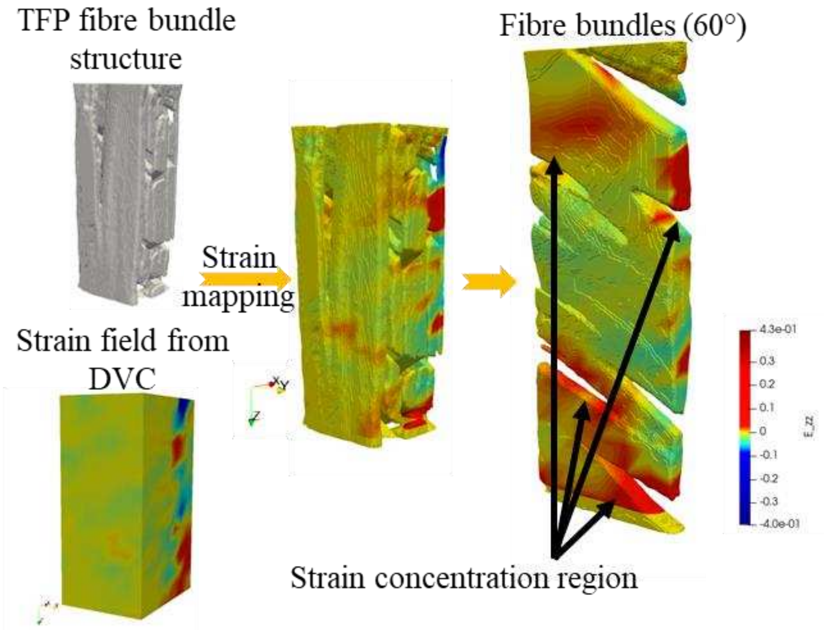

Figure 8: The strain field (ε_{zz}, along the loading direction) mapped onto the special fibre bundle structure of the TFP composite sample under tension.

4.2 Internal deformation of the TFP composite under tension

The internal deformation of the TFP composite structure was characterised through strain maps obtained using the G-DVC method. The mesh size was selected as 31 voxels from a sensitivity analysis. The strain field obtained from DVC results was mapped onto the fibre bundle structure of the TFP composite. The distinct fibre bundle structure was caused by the stitch thread used in the TFP process. As can be seen from Figure 8, the strain concentrations were located near the resin-rich zones in the 60° orientation fibre bundle. These resin-rich zones were created by the stitch threads with local strain values up to 43% recorded by DVC. These quantified local strain values can help understand the formation of cracks observed at the interface between fibre bundles and resin-rich regions in TFP composite loaded under tension.

5. CONCLUSIONS

The developed Python-coded DVC program provides high efficiency, easy-operation, and accuracy for the correlation of in-situ CT results with high rigid body motion. The developed methodology offers new opportunities for a better understanding of complex damage development in TFP composites as well as validation means for multiscale models aimed at predicting their mechanical response.

6. REFERENCES

1. Sun, G., Mitchell, R., Chen, Z., Omrani, F., Smith, M., Fairclough, J.P.A. and Pinna, C., 3d characterisation of the tensile failure of CFRPS manufactured through tailored fibre placement. *Proceedings ICCM 23, Belfast, United Kingdom.*

2. Almeida Jr, J.H.S., Bittrich, L., Nomura, T. and Spickenheuer, A., 2019. Cross-section optimization of topologically-optimized variable-axial anisotropic composite structures. Composite Structures, 225, p.111150.
3. Gliesche, K. and Feltin, D., 1997. Preforms for composite parts made by tailored fibre placement. Proceedings ICCM-11, Gold Coast, Australia, 5, pp.17-26.
4. Uhlig, K., Spickenheuer, A., Bittrich, L. and Heinrich, G., 2017, August. Tailored fiber placement based on epoxy preimpregnated carbon rovings (Towpreg). In Proceedings of the Twenty-first International Conference on Composite Materials, Xi'an, China (pp. 20-25).
5. Spickenheuer, A., Leipprand, A., Bittrich, L., Uhlig, K., Richter, E. and Heinrich, G., 2014, June. Process-dependent material properties for structural simulation of composites made by tailored fibre placement. In Proceedings of the ECCM16-16th European conference on composite materials (June, 22-26, 2014, Seville, Spain).
6. Bay, B.K., Smith, T.S., Fyhrie, D.P. and Saad, M., 1999. Digital volume correlation: three-dimensional strain mapping using X-ray tomography. Experimental mechanics, 39, pp.217-226.
7. Wan, F., Liu, R., Wang, Y., Cao, Y., Zhang, C. and Marrow, T.J., 2019. Damage development during flexural loading of a 5-directional braided C/C-SiC composite, characterized by X-ray tomography and digital volume correlation. Ceramics International, 45(5), pp.5601-5612.
8. Brault, R., Germaneau, A., Dupré, J.C., Doumalin, P., Mistou, S. and Fazzini, M., 2013. In-situ analysis of laminated composite materials by X-ray micro-computed tomography and digital volume correlation. Experimental Mechanics, 53, pp.1143-1151.
9. Mehdikhani, M., Breite, C., Swolfs, Y., Soete, J., Wevers, M., Lomov, S.V. and Gorbatikh, L., 2021. Digital volume correlation for meso/micro in-situ damage analysis in carbon fiber reinforced composites. Composites Science and Technology, 213, p.108944.
10. Pan, B. and Wang, B., 2020. Some recent advances in digital volume correlation. Optics and Lasers in Engineering, 135, p.106189.
11. Pan, B., Li, K. and Tong, W., 2013. Fast, robust and accurate digital image correlation calculation without redundant computations. Experimental Mechanics, 53, pp.1277-1289.
12. Pan, B. and Wang, B., 2017. A flexible and accurate digital volume correlation method applicable to high-resolution volumetric images. Measurement Science and Technology, 28(10), p.105007.
13. Dragonfly 2022.2 [Computer software]. Comet Technologies Canada Inc., Montreal, Canada; software available at https://www.theobjects.com/dragonfly.
14. Ahrens, James, Geveci, Berk, Law, Charles, ParaView: An End-User Tool for Large Data Visualization, Visualization Handbook, Elsevier, 2005, ISBN-13: 9780123875822
15. Mostafavi, M., Collins, D.M., Cai, B., Bradley, R., Atwood, R.C., Reinhard, C., Jiang, X., Galano, M., Lee, P.D. and Marrow, T.J., 2015. Yield behavior beneath hardness indentations in ductile metals, measured by three-dimensional computed X-ray tomography and digital volume correlation. Acta Materialia, 82, pp.468-482.

16. Lee, S., Jo, E. and Ji, W., 2020. Digital volume correlation technique for characterizing subsurface deformation behavior of a laminated composite. *Composites Part B: Engineering*, *194*, p.108052.